

Visualization Measurements of Vortex Flows

Martin V. Lowson*

University of Bristol, Bristol, England, United Kingdom

Novel flow visualization experiments have been used on the separated vortex flow on a delta wing at low speed ($3000 < Re_c < 30,000$) to give measurements of flow parameters for comparison with theory. Data on vortex core position, vortex sheet shape, vortex strength, and local velocity magnitude and direction in the core have been determined. The results show surprising consistency with several features of established theoretical models for high Re flows and further justify the use of low Re experiments for vortex flows. The results also indicate areas where care should be taken in extrapolating results at low Re to flight cases.

Introduction

THE vortex flow over a delta wing is an example of a flow that is thought to be controlled by inviscid fluid effects. Under these conditions, results obtained at low speeds can offer significant insights for basic phenomena in higher speed flows. The flow is also a model for a class of complicated separated flows dominated by vortex effects, and one for which a variety of theoretical models exists. In the present work, a series of flow visualization experiments have been undertaken on the vortex flow over slender delta wings at low speeds. The objective has been to obtain quantified measurements of the flow, and, in particular, measurements of streamline shape and local velocities in order to make comparisons with theory based on inviscid vortex sheet models.

The formal basis for such models of the separated flow is the high Reynolds number approximation when the convective terms in the Navier-Stokes equations are much larger than the diffusive terms. Under these conditions the effects of diffusion, whether viscous or turbulent, are confined to a thin shear layer. In practice, the diffusive terms only reduce in scale slowly in comparison to the convective terms for turbulent shear layers, so that at any practical Reynolds number the approximation has limited validity.

The best known theoretical model for the separated flow on a slender wing is due to Mangler and Smith,¹ which reached its definitive form in the paper of Smith.² However, all of the models for the flow take a similar approach, in which the separated shear layer over the wing is modeled by a combination of concentrated vortex and feeding vortex sheet. The magnitude of the vortex parameters are determined by fluid dynamic conditions on the sheet in combination with a Kutta condition at the leading edge. Reasonable agreement with experiment for vortex core position, and for pressure distributions and other aerodynamic measurements, has been shown.

This agreement, however, is by no means exact. There are uncertainties about the nature and influence of the "secondary" separation that occurs beneath the main feeding sheet near the leading edge. There are also unexpected features of the vortex core, the most spectacular of which is vortex breakdown—Peckham³—causing a major disruption of the separated flow towards the rear of the wing at sufficiently large angle of attack.

Nevertheless, it has been demonstrated that experiments at low speeds on such flows can provide significant information about higher speed flows. Vortex core position has been demonstrated to be only modestly affected by major changes in Reynolds number. Much of the information on vortex breakdown has continued to come from laboratory experiments at low Re . Recently, Campbell et al.⁴ have shown that full-scale visualization of flowfields on fighter aircraft at high angle of attack reveals detailed flow structures that are similar to those previously seen in laboratory studies.

The principal motivation for the present work was the realization that tests at sufficiently low speeds might give clear visualizations of streamline shape that could be compared with existing theories for vortex sheets. It is thought that flow visualization should be used not merely as an aid to understanding but as a measurement technique in its own right. This approach is already established for flows on highly swept wings for the determination of vortex position and vortex breakdown position. Visualization techniques can provide information about the whole flow, rather than the part of the flow where a probe is located, and are thus potentially excellent measurement tools. The key is the introduction of the visualization medium into the flow at the best location. In the present case, smoke has been introduced along the whole leading edge of the wing and, thus, is swept into the shear layer, enabling direct measurement of streamline shape and position. The investigations reported here have been undertaken at speeds where the flow has been laminar or transitional in nature. It has been found that this regime affords several additional opportunities for using visualization as a measurement tool.

Experiments

The experiments were mounted in the 0.8-m \times 0.6-m closed return wind tunnel at the University of Bristol. The tunnel has been specially designed with a contraction ratio of 12:1 to produce flow of low turbulence, and a turbulence level of $< 0.05\%$ is achieved. The normal working range of the tunnel is 1–100 m/s, but where necessary for the present work, a lower speed was obtained by inserting a high-blockage (87%) peg board immediately behind the working section. This permitted the achievement of velocities down to 0.09 m/s in the working section and retained low turbulence ($< 0.1\%$), albeit with some flow unsteadiness. Flow speeds were measured with a commercial hot-wire meter, calibrated against a vane anemometer.

The model used consisted of a delta wing of 70-deg leading-edge sweep and 44.1-cm chord. The wing had a sharp leading edge beveled at 20 deg on the underside. Overall thickness was 1.2 cm. The wing was mounted on a parallel arm arrangement, so that incidence could be easily varied from outside the tunnel. The same mechanism also carried the camera when aligned for shots looking directly up the wing.

Presented as Paper 89-0191 at the AIAA 27th Aerospace Sciences Meeting, Reno, NV, Jan. 9–12; received March 3, 1990; revision received July 5, 1990; accepted for publication July 5, 1990. Copyright © 1990 by the American Institute of Aeronautics and Astronautics, Inc. All rights reserved.

*Professor, Department of Aerospace Engineering. Associate Fellow AIAA.

The principal flow visualization medium was smoke, formed from mineral oil drops on a hot plate. The smoke was passed up a tube to a plenum chamber within the model by pressure from a gas bottle. The smoke outlet on the model was a slit 0.2 mm wide, uniformly machined 1 mm below the whole leading edge, passing into the plenum chamber. By this means, a uniform sheet of smoke was introduced almost directly into the vortex sheet leaving the leading edge. For certain tests, to be described later, the smoke supply was blocked off at regular intervals down the leading edge with masking tape. Testing by introduction of excessive smoke demonstrated that there was no observable distorting effect on the flow under nearly all circumstances. The exception was at very low speeds (< 0.1 m/s), when reduced smoke levels were used to avoid flow disturbance.

The flow was illuminated with a variety of sources. An argon ion laser (nominally 5 W) operating in all lines mode at around 8 W was used to produce a light sheet via a small cylindrical lens. An optical bench setup provided beam steering to achieve a light sheet of specific height and chordwise position. The light sheet could also be placed at a prescribed angle of incidence in the tunnel and, for the majority of the work, was inclined at 90 deg to the wing surface. Flash and flood light was also used, along with stroboscopic illumination.

Photography was accomplished with a variety of cameras, principally a 35-mm camera with motor drive. Most of the laser pictures have been taken at an exposure of $1/2000$ s at F3.5 on 400 ASA film developed to produce 3200 ASA. Some cine-photography was also undertaken. The tunnel was liberally provided with windows so that views could be taken from above or to the side of the model. For the laser light sheet work, the camera was positioned on the axis of the model within the wind tunnel on an extension to the parallel arm mechanism. This enabled undistorted pictures of the flow

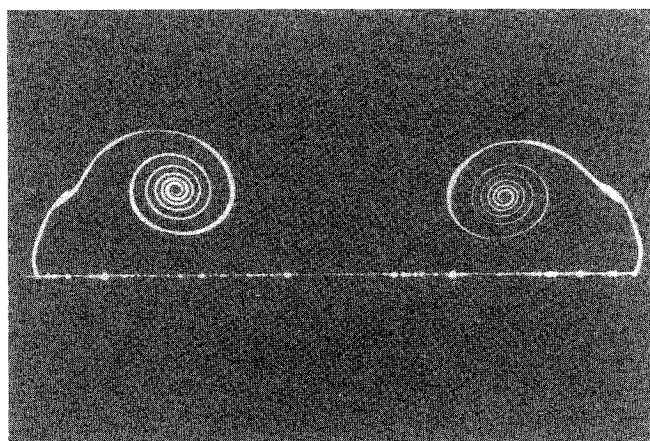
to be taken and, thus, permitted measurements to be taken from the photographs.

For some of the experiments, the flow was excited. This was achieved either by vibration or with a loud speaker mounted in the tunnel wall downstream of the model.

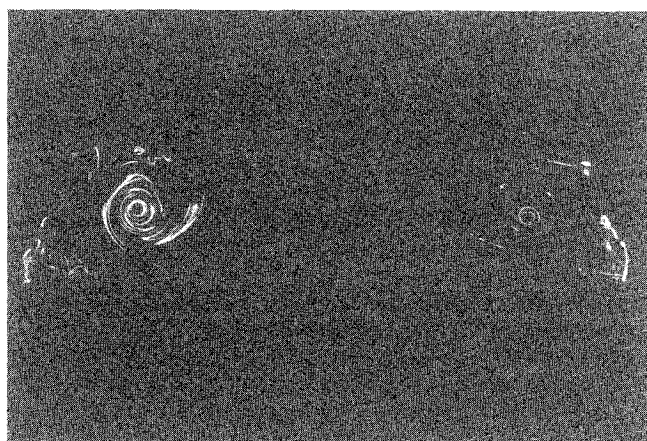
Initial Results

Typical results of the laser light sheet visualizations of the flow are shown in Fig. 1. It can be seen that, at sufficiently low speed, the flow is laminar and provides an excellent visualization of the streamline shape. As speed is increased, the flow becomes unsteady, generating vortex structures within the separated free shear layer, and finally becomes fully turbulent. An analysis of the process of transition to turbulence in this separated shear layer has been made in another paper, Lowson,⁵ and will not be discussed in detail here. However, from the viewpoint of the present paper, the key feature is that the appearance of transitional and then turbulent flow obscures the detail of the shape of the feeding sheet in the photographs. Other features of these flows will be discussed later in the paper.

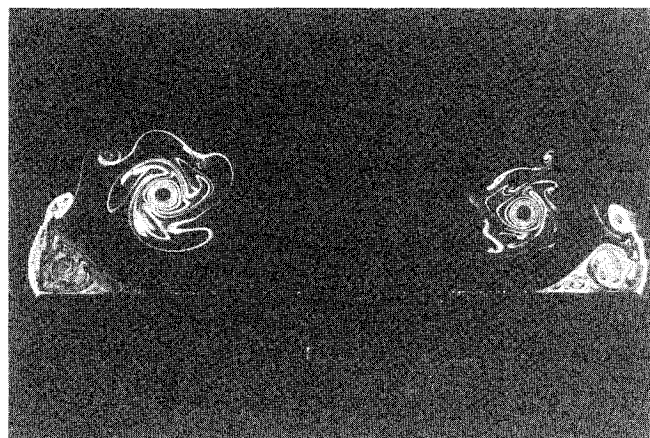
The first check made on the results was that the flows studied were indeed typical. Measurements were made of the vortex core position from photographs of the flow at various angles of attack. The results (shown in Fig. 2) are compared with those from several other investigators, based on data from Smith,² but with some additional points. The results are plotted as position as a proportion of local semispan vs α , the ratio of angle of attack to semiapex angle. These are the correlating parameters given by slender body theory. The core lies approximately along a straight line. When this is the case, a single point arises per test condition. However, in some experiments the core was not straight, and in these cases, the position at half-chord has been plotted, following Smith.² The



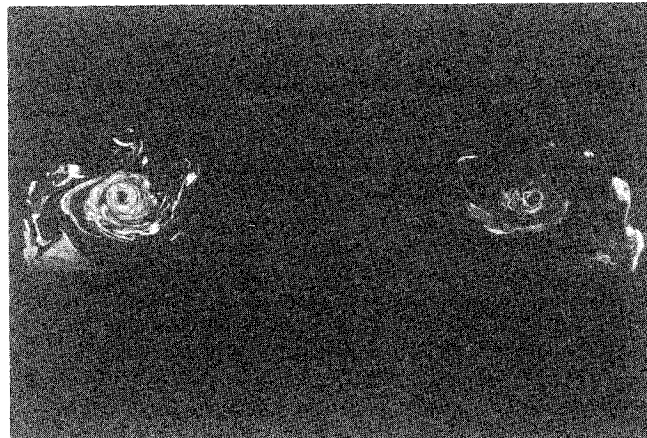
a) 0.22 m/s



c) 0.82 m/s



b) 0.72 m/s



d) 1.36 m/s

Fig. 1 Laser light sheet visualization at 20-deg incidence.

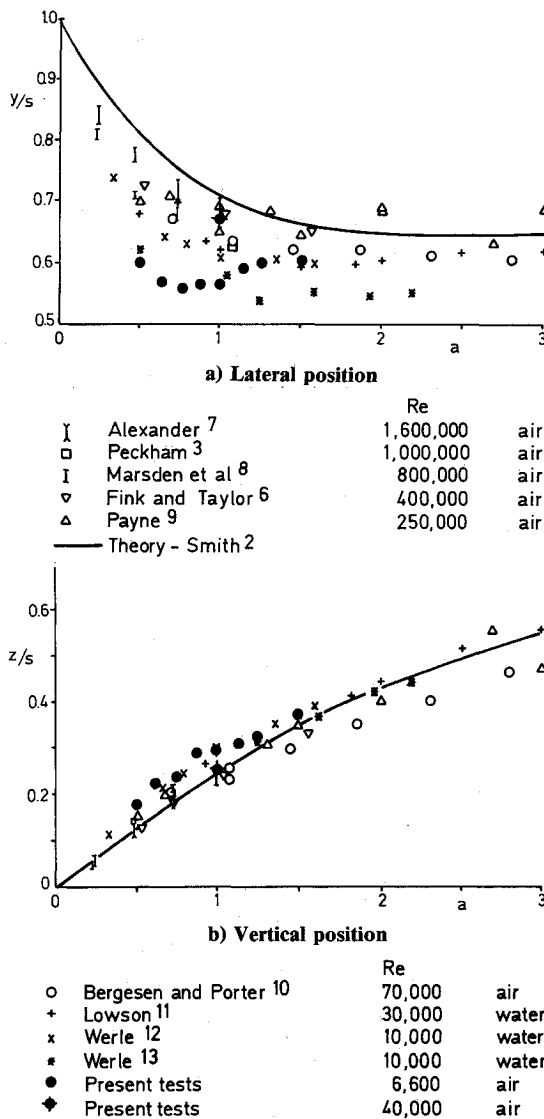


Fig. 2 Correlation of vortex core position from various observations.

cases where a range of core positions are shown correspond to cases where differing methods of measurement gave different results for core positions.

It can be seen that the vortex core positions measured by a variety of investigators on wings of various sweep angles show broad agreement when compared in this way and show reasonable agreement with theory, but there is some scatter. The principal factor causing this scatter is Reynolds number, and the value of Re based on overall wing chord is noted for each case. A major difference in previous work has been between water-tunnel and wind-tunnel results. It can be seen that the water-tunnel vortex locations are generally further inboard and somewhat higher away from the wing. This is believed to be due to the effects of the large laminar secondary separation that displaces the vortex inboard and slightly upward.

It will also be observed that the present wind-tunnel results at low speed show broad agreement with the previous water-tunnel results. This is to be expected because the Reynolds number of the tests is more comparable with the previous water-tunnel than wind-tunnel results. One other point to emerge from the present correlations is that the effect of Re appears to be reduced at higher values of a . This is consistent with the smaller extent of secondary separation observed at higher angles of attack.

Several investigators have found that transition in the secondary separation results in an outboard movement of the

vortex cores. The wind-tunnel results from other investigators given in Fig. 2 almost certainly correspond to this situation. In the present case, Fig. 1d shows that at a speed of 1.36 m/s the secondary separation is turbulent. The reduced scale of this part of the flow is associated with an outboard movement of the vortex core, as can be seen by inspection of the visualizations. The effect is indicated in Fig. 2 ($a = 1$). The vortex core position in this case virtually overlays the results of Fink and Taylor⁶ for the same configuration at a much larger Reynolds number, but at an equivalent state of the secondary separation. Thus, it may be concluded that the present experiments offer acceptable continuity with previous results, both for laminar and turbulent secondary separations.

It is interesting that transition in the separating shear layer does not of itself appear to cause a major difference in the gross vortex flow parameters. However, Smith² points out that many wind-tunnel experiments still involve laminar boundary layers on the wing. The appearance of turbulence in the wing boundary layer before the shear layer leaves the leading edge causes a further outboard movement of the vortex and is presumably the condition at full scale.

One other possible reason for a divergence in vortex position is the spanwise camber inherent in the present model geometry. However, this effect would be small. A further known effect is the effect of thickness, but the present models have an overall t/c of 2.7% and can be classified as thin for the purposes of this comparison.

Analysis of Vortex Sheet Shape

The clarity of the visualization allows direct measurement of streamline shape. Before analyzing the shape, it is of interest to examine possible simple geometries. Although various models are available in the literature, it seems desirable to start from first principles and seek a shape that matches the conical nature of the flow. Thus, a shape is sought that was identical from section to section apart from a scale change. The only free parameter is the angle around the spiral, (Θ) , so it would appear that a function $r(\Theta)$ is required for which multiplication by an arbitrary factor F is equivalent to a change of angle ϕ :

$$F r(\Theta) = r(\Theta + \phi) \quad (1)$$

The simplest function that satisfies this relation is

$$r = A \exp(\Theta/\Theta_0) \quad (2)$$

Thus, it could be argued that the exponential spiral is the natural conical spiral form. Alternative functional forms are available from other theories (e.g., the reciprocal spiral of Mangler and Smith¹).

The length of the exponential spiral between any two points at radii r_1, r_2 is given by

$$s = 2\pi S(r_1 - r_2) \quad (3)$$

where S is a "stretch factor" for the spiral. In terms of the parameters used above

$$S = (\Theta_0^2 + 1)^{0.5} \quad (4)$$

A notable feature of the exponential spiral is that even though it wraps infinitely many times as it approaches the origin, the spiral is of finite length. In analyzing the experimental shape, the principal difficulty is the unknown origin of Θ . In order to get around this, Δr is plotted against r , taking Δr as the change in radius over one turn of the spiral. The result of a log-log plot is shown in Fig. 3. It is straightforward to turn the power law resulting from analysis of Fig. 3 into an expression for r in terms of Θ , and vice versa. The Mangler and Smith law of $r = \Theta^{-1}$ gives Δr proportional to r^2 , whereas the exponential law gives Δr proportional to r .

Figure 3 shows that the square law fit of Mangler and Smith only applies over the outer loop of the spiral. A linear law could be considered. A direct fit produces an $r^{0.58}$ law. However, these approaches involve differencing and are, therefore, subject to error magnification.

To test a possible exponential law, a direct plot of $\log r$ vs θ can be used. This is shown in Fig. 4. It is most interesting that a reasonable straight line plot emerges. The divergencies at small and large r are not unreasonable. The outer arms of the sheet would not be expected to conform exactly to simple laws, whereas the inner core is the part most affected by viscosity.

The same exponential shape was found for all cases in which the streamlines were sufficiently well defined to permit measurement. As shown in Fig. 1, at higher speeds (> 0.6 m/s in these initial experiments) the flow goes unstable and eventually completely turbulent in the outer loops, so that it is not possible to obtain precise data on shape. Thus, the experiments appear to support an exponential spiral shape for the streamlines over a delta wing at low speeds. While the sharpness of the smoke trace at these speeds demonstrates that relatively little particle diffusion has taken place, momentum exchange due to viscous effects will still occur.

It is also possible to make direct comparisons of streamline shape with experiment. These are shown in Fig. 5. Figure 5a gives a comparison of various equivalent results centered on the vortex core. The principal comparison is between a trace from the present low-speed experiment (Fig. 6) and a theoretical result for a vortex sheet. The theoretical result is taken from Barsby,¹⁴ which is essentially the result of Smith² ex-

tended for a further turn around the core. For comparison, part of a total head survey from Fink and Taylor⁶ is also shown.

Figure 5b gives similar comparisons scaled on the local span to provide information on the shape of the feeding sheet. For this, a different case (original visualization not shown) with a larger ratio of angle of attack to semiapex angle was chosen in order to minimize the effects of the secondary separation. The close agreement in the shape of the feeding sheet between the present low-speed visualizations and the total head surveys at higher Re is noteworthy. Both the visualizations and the surveys appear to disagree with the theoretically predicted shape at this condition.

Figures 5a and 5b also demonstrate that the overall scale of the vortex flow remains the same with variation of Reynolds number and is generally consistent with the theoretical predictions. This is a little surprising and indicates that inviscid mechanisms may dominate the larger scale features.

Further Data

The preceding exponential spiral arguments are purely geometric and give no kinetic information on the flow. In order to provide more data on the vortex sheet parameters, the smoke supply was interrupted at regular intervals down the leading edge, thus providing "antismoke." The resulting gaps in the smoke pattern feed into the core, as shown in Fig. 6, and enable the point of origin of various parts of the streamline to be identified. The length of the smoke trace between successive gaps can also be measured on photographs of the laser light

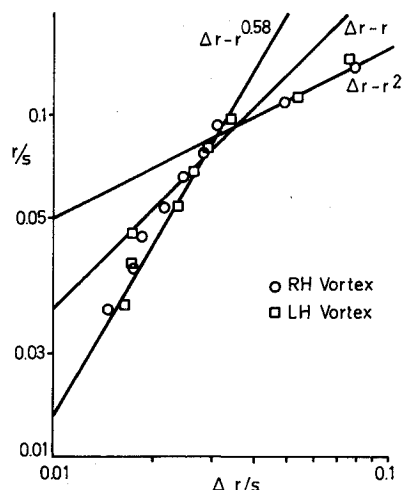


Fig. 3 Log-log plot of streamline shape.

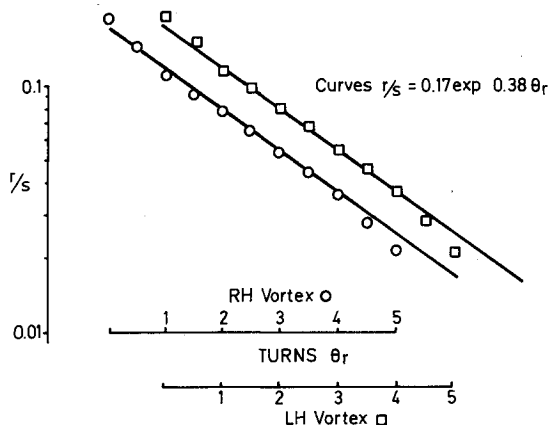


Fig. 4 Log linear plot of streamline shape 0.22 m/s at 20-deg incidence.

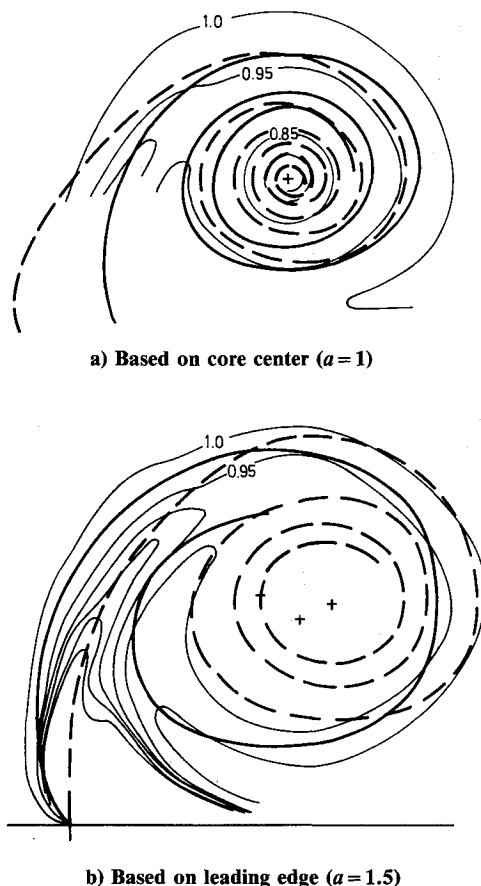


Fig. 5 Comparison of vortex sheet shapes.
— Total Head Survey Fink and Taylor⁶
--- Present Visualisations
— Theory Smith², Barsby¹⁴

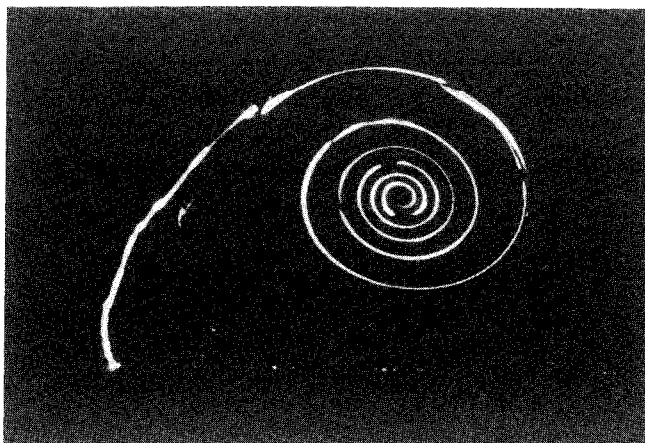


Fig. 6 Visualization at 20-deg incidence; 0.24 m/s, 0.75 chord with interrupted smoke.

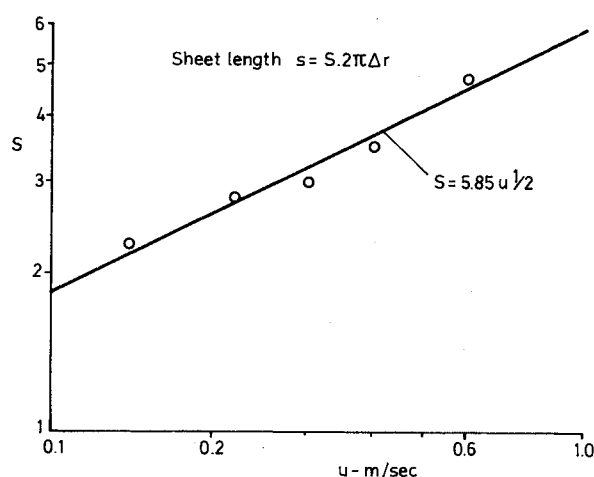


Fig. 7a Streamline stretch factor vs velocity.

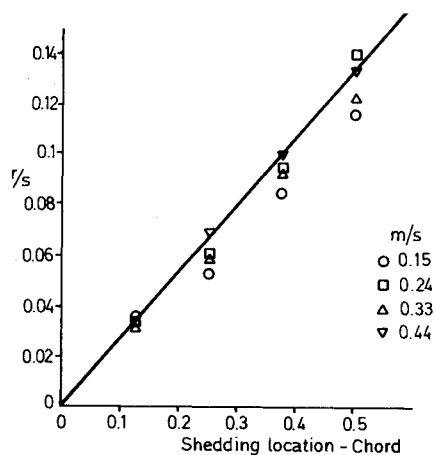


Fig. 7b Position in core vs shedding location.

sheet visualization, thus providing a measure of the relative stretching occurring in various parts of the vortex core.

The results were surprising. The length of smoke trace between each gap was found to be the same, showing that little stretching occurred within the vortex cores in these experiments. Thus, most of the stretching occurs in the feeding sheet before it merges into the wrapped vortex core. The magnitude of the velocity in the streamline itself is found to be almost constant throughout the core. Angular velocity increases toward the center because of the reduction in radius and the infinite wrapping process mentioned previously.

The actual stretching has been found to be a function of velocity, with the vortex undergoing a tightening and an in-

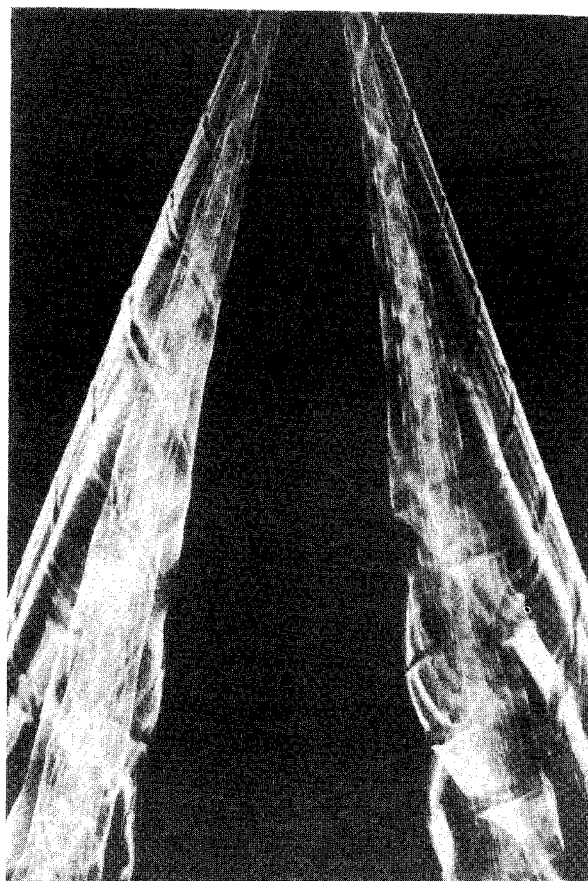


Fig. 8 View of flow from above showing spiral streamlines and internal smoke structure; 0.33 m/s, 20 deg.

crease in the number of turns as velocity is increased. There are several possible descriptive parameters. For example, the distance between gaps in the smoke supply could be measured, or the actual length of rolled streamline measured, directly from photographs. Both of these approaches were used and gave equivalent results. However, it was found that the most suitable descriptive parameter is a "stretch factor," defined by the length of the sheet over one turn divided by the change of radius over another turn. This parameter is constant for an exponential spiral and gives a measure of its tightness. It can readily be measured from the laser light sheet photographs by matching an exponential spiral to the shape and determining the appropriate constant.

A plot of this stretch factor vs velocity is given in Fig. 7a. It will be noted that the variation with velocity corresponds to a half-power law. This matches the viscous-dominated nature of the vortex core in the present experiments. Figure 7b gives a plot of the radial location in the core of material leaving various stations on the leading edge. This was determined by measurement of the location of the interruptions in the trace in laser light sheet visualizations at 0.75 chord, and the x axis corresponds to proportions upstream of this location. It will be observed that there is little effect of speed. This is consistent with a uniform increase of stretching with speed over the whole of the shear layer leaving the leading edge. More detailed studies would probably indicate a variation along the leading edge consistent with Re based on local chord, but the present methods do not permit the flow at the smallest values of local Re close to the apex to be visualized. The experiments do demonstrate a gradual loosening of the spiral as it passes down the wing, but this may be in part due to the effects of the trailing edge.

Flash photography of the flow has revealed further information about the nature of the rolled up vortex sheet. A typical result is shown in Fig. 8. It can be observed, especially on

the LH core, that each of the streamline "antismoke" traces from the leading edge rolls into a spiral form within the overall vortex structure. Measurements of any one spiral shows that each trace is approximately cylindrical. This was also observed by Lambourne and Bryer.¹⁵ Thus, after the leading-edge material is taken into the core, it continues down the core at a constant radius from the core axis. The conical vortex sheet in these experiments is an assembly of spiral streamlines. This result is also consistent with the exponential model for vortex core shape.

Measurements can be made of the relative magnitude of axial and circumferential components in the core. For the case, shown in Fig. 8, of 20-deg angle of attack, the ratio of u/v is 1.33 and is approximately constant through the core.

Shear-Layer Instabilities

The visualizations have also revealed the presence of instabilities in the shear layer. The existence of quasi-two-dimensional shear-layer instabilities parallel to the leading edge, first noted by Gad-el-Hak and Blackwelder¹⁶ has been confirmed (Fig. 9). A second steady, and locally streamwise, instability of the feeding shear layer was also found. This gave rise to cellular structures in the vortex core, as observed by Payne⁹ and Payne et al.,¹⁷ and is illustrated in the present paper in Fig. 1b. Details of the instability process have been given in Lawson.⁵ The second instability is only of peripheral interest to the present paper, but a description of the first instability is necessary since it has been found possible to use it as a measurement tool.

The two-dimensional instabilities springing from the leading edge develop into vortices within the feeding sheet, which then combine through a pairing mechanism. A second pairing is also observed at tunnel speeds above 0.25 m/s. The overall ef-

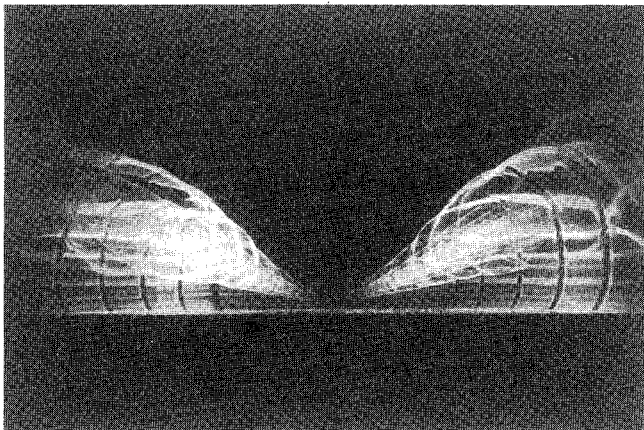


Fig. 9 View on wing axis showing sheet instabilities at 50 Hz; 0.33 m/s, 20 deg.

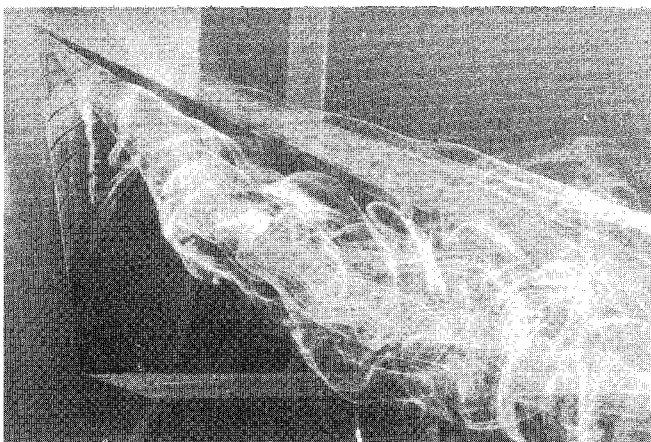


Fig. 10 Overall view of vortex flow development at 0.33 m/s, 20 deg.

fect on the flow can be seen in Fig. 10. The actual pairing process has been found to be highly complex, as in other examples of the mechanism, e.g., Winant and Browand.¹⁸ In the present case, conical flow, combined with the model geometry, ensures that the shear-layer conditions are uniform on leaving the leading edge. However, the shear layer rolls up proportionally more quickly toward the apex because of the absolute scale. It appears that this vortex stretching and roll-up process has a strong stabilizing effect on the flow and inhibits the pairing mechanism. Increase of speed is destabilizing.

The result is that the forward part of the flow is relatively uniform and stable, whereas it becomes progressively more unstable toward the trailing edge, eventually becoming turbulent. The transition process moves up the wing with speed.

A remarkable consequence of this effect is that the instability waves that start in the shear layer near the apex are carried into the center of the vortex core without further development, leading to regular smoke concentrations along the core center, see Fig. 8. Indeed, the RH core of this photograph shows how the outer arms of the spiral sheet contain concentrations at double, and eventually quadruple, the spacing at the center. This is believed to be due to the stabilization of paired vortices by a combination of convection, stretching, and viscosity as they are carried into the core.

Gad-el-Hak and Blackwelder found the instability to be associated with a frequency that varied with speed. In the present experiments, it was initially found that the forcing frequency was constant. Many investigators (cf. Ho and Huerre¹⁹) have found that the shear layer is unstable to a wide range of frequencies and to remarkably small levels of vibrational input. It was determined that in the present experiments the shear layer was reacting to vibrational inputs of 0.02 g associated with the tunnel motor cooling fan running at a constant speed of 50 Hz. This excitation is present for all figures in the present paper except Figs. 1b and 11.

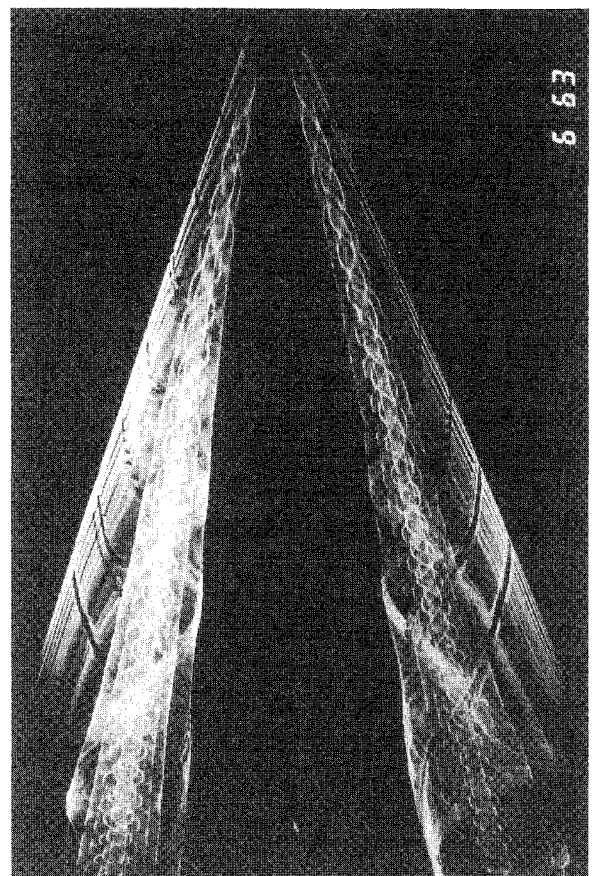


Fig. 11 View of flow from above showing internal smoke structure; 0.22 m/s, 20 deg, 20-Hz excitation.

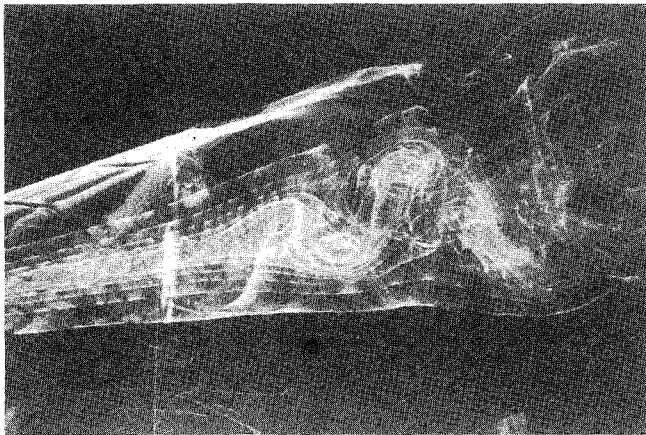


Fig. 12 Vortex breakdown at 25-deg incidence, 0.33 m/s.

Since the initial shear-layer instability is convected into the vortex core, this frequency is also associated with the smoke concentrations that can be seen in Fig. 8. Stroboscopic analysis has demonstrated that the whole of the associated internal structure, even in the wake, is locked to the same frequency. An example is shown in Fig. 11 of a flow excited at 20 Hz. This is at a lower speed, and forcing frequency pairing has been inhibited over most of the rolled-up vortex. It may also be noted that theory and experiment have demonstrated that under the circumstances of the present experiments the convection velocity of these instabilities/vortices is at the local mean speed of the shear layer.

The preceding observations suggest that direct measurement of flow velocities within the vortex core can be made via measurement of the separation of the structures within it. This approach has been tested in the present case by measurements taken on flash photographs of the flow. The result gives a sum of axial and circumferential velocities within the core. However, by combining this result with knowledge of the local flow direction from the "antismoke" traces described, the magnitude and direction of the velocity may be determined.

For the example shown in Fig. 8, this has given an overall magnitude of 0.48 m/s, for this 0.33 m/s freestream case. Note that the measurement has also given an independent verification of the approximate constancy of the velocity in the sheet within the core, as demonstrated by earlier analysis of the stretching process.

The ability to measure the velocity within the vortex core by simple nonintrusive photographic methods is thought to be of wider interest. The methods give results at positions that may be directly related to the observed features of the flow, e.g., the vortex core. Note that it is possible under some circumstances to obtain finer spatial resolution with the present techniques than is available in either hot-wire or laser doppler anemometry. This is particularly well matched to tightly wound shear layers.

Some work has also been undertaken on the vortex breakdown phenomenon. Figure 12 shows how the vortex sheet structure is wrapped around the spiral vortex breakdown form. It would also be possible to measure velocities from the concentration spacings in this case, although this has not been done at present. Nevertheless, the picture does demonstrate the orderly nature, and much of the detail, of vortex breakdown in this case. The picture also shows the independence of the vortex breakdown from feeding sheet instabilities, a mechanism suggested by some previous authors.

Discussion

The original intention of the present experiments was to measure the shape of the shed vortex sheet experimentally. However, it can be seen that the streamline shapes measured in the laminar flow regime at low Reynolds number, $Re = 6600$, are almost certainly strongly affected by viscosity. Thus, it

would be unreasonable to expect correlation with a vortex sheet theory based on the high Reynolds number approximation. Although the present tests are well removed from practical flight Reynolds numbers, they do correspond to test conditions that have been widely used for flow visualization studies of separated flows, for example, in water. Thus, a more detailed understanding of the divergencies from theory and full-scale data is of interest.

The original paper by Mangler and Smith¹ gives, in addition to a theoretical shape, a prediction for the velocity distribution in the core, which does not seem to have been explicitly noted by subsequent writers. Mangler and Smith predict that the transverse velocity is uniform, i.e., independent of radius, as found in the present experiments. Since in any fluid flow the velocity distribution is of more practical importance than the particle paths, this agreement between a high Re theory and low Re experiment is significant.

A consequence of a uniform transverse velocity distribution is that the overall vortex strength is simply a multiple of that velocity by the linear dimension of the core. Thus, the fact that the core size in the present experiments is similar to that predicted by theory and also in experiments at higher Re implies that the nondimensional vortex strength is also consistent. An estimate of vortex strength can be made. For the case studied here, taking a typical core size of $r/x = 0.05$ gives a value for $\gamma = \Gamma/2\pi U_\infty$ of 0.50, which compares to the Mangler and Smith figure of 0.54. This agreement is encouraging, but it must be emphasized that it is a single point from a preliminary set of experiments.

Difficulties do appear as speed is increased. As already shown in Fig. 7a, the vortex sheet "stretch factor," which gives a direct measure of transverse velocity, increases as $U^{0.5}$. However, this only applies to the laminar core, which reduces in size as velocity increases. Outside this core there is considerable unsteadiness, as shown by the laser light sheet visualizations, which prevents any clear statement being made about velocity or vorticity distributions. It should also be noted that experiments at higher speeds by, for example, Earnshaw,²⁰ Verhaagen and Kruisbrink,²¹ and Kjølgaard (NASA Langley, private communication), do not find a uniform transverse velocity distribution.

A further divergence between the present results and experiments at higher speeds is in the axial velocity profiles in the laminar core. In particular, it is usually found, as in the experiments referenced earlier, that there is a marked increase in velocity close to the core center. This is consistent with the theories of Hall²² and Stewartson and Hall.²³ In the present tests, an increase in axial velocity in the vortex is found, but this was uniformly distributed over the whole of the core.

At the low Re of the present tests, viscous effects must be expected to dominate. The original theory of Hall²² for the viscous core showed a reduction of core axial velocity with Re , but accuracy was only claimed down to Reynolds numbers based on local chord of 10^5 . The subsequent work of Stewartson and Hall²³ gave an explicit but complex asymptotic expansion for the viscous flow for which the leading term in the core axial superequilibrium had the form $\chi^{-1} \log \chi$. The parameter χ is of order unity for the flow studied above, suggesting zero superequilibrium in the core due to the effects of viscosity. Thus, although the experiment is outside the range of application of the theory, the results do match the theoretical suggestions.

Flows at the low Reynolds numbers of the present tests inevitably have core conditions that are not representative of those at higher Reynolds numbers. In addition to the differences noted previously, it will be recalled that the consequences of the large laminar secondary separation and of the laminar rather than turbulent boundary layer on the wing are also effects that need to be considered in any extrapolation from low-speed to flight cases.

However, from the present experiments it can be seen that many of the important flow parameters, such as vortex core position, vortex strength, and vortex core size, show accep-

table agreement with higher speed results. Thus, it appears that the essential features of the separated vortex flow are maintained even at low Re . The present results serve to throw more emphasis on the leading-edge conditions and such features as secondary separation as the determining factors for the flowfield.

Conclusions

Novel flow visualization techniques have provided new information about the vortex flows over a delta wing at low Reynolds numbers ($Re_c = 6600$). In the present experiments, in the laminar/transitional regime, the results suggest the following.

- 1) Streamline shape in the crossflow plane corresponds to an exponential spiral.
- 2) Velocity magnitude in the core is approximately constant.
- 3) Stretching of the shear layer occurs before it wraps around the core.
- 4) The conical shear layer consists of a set of approximately cylindrical spiral streamlines.
- 5) Shear-layer instability and associated vortex pairing are inhibited by the vortex wrapping process.
- 6) The frequency of the resulting vortex structure within the core can be fixed so that measurements of the structure can provide direct estimates of local velocities, potentially even for vortex breakdown.
- 7) The velocity distribution and vortex strength are consistent with the theoretical predictions for a high Re model.
- 8) The results appear to provide justification for low Re studies of high Re separated vortex flows and suggest areas where care will be required in extrapolation from low to high Re .

Acknowledgment

I would like to thank J. H. B. Smith for helpful comments on the results.

References

- ¹Mangler, K. W., and Smith, J. H. B., "A Theory for the Flow Past a Slender Delta Wing with Leading Edge Separation," *Proceedings of the Royal Society A*, Vol. 251, 1959, pp. 200-217.
- ²Smith, J. H. B., "Improved Calculations of Leading Edge Separation from Slender Thin Delta Wings," *Proceedings of Royal Society A*, Vol. 306, 1968, pp. 67-99; also RAE TR 66070, Mar. 1966.
- ³Peckham, D. H., "Low Speed Wind Tunnel Tests on a Series of Uncambered Slender Pointed Wings with Sharp Edges," Aeronautical Research Council, ARC R&M 3186, 1958.
- ⁴Campbell, J. F., Chambers, J. R., and Rumsey, C. L., "Observation of Airplane Flow Fields by Natural Condensation Effects," AIAA Paper 88-0191, Jan. 1988.
- ⁵Lowson, M. V., "The Three Dimensional Vortex Sheet Structure on Delta Wings," Paper 11, AGARD Symposium on Fluid Dynamics of Three Dimensional Shear Flows and Transition, Oct. 1988.
- ⁶Fink, P. T., and Taylor, J., "Some Low Speed Experiments with 20 Degree Delta Wings," Aeronautical Research Council, ARC R&M 3489, 1955.
- ⁷Alexander, A. J., "Experiments on a Delta Wing using Leading-Edge Blowing to Remove the Secondary Separation," College of Aeronautics, Cranfield, Rept. 161, 1963.
- ⁸Marsden, D. J., Simpson, R. W., and Rainbird, W. J., "The Flow over Delta Wings at Low Speeds with Leading Edge Separation," College of Aeronautics, Cranfield, Rept. 114, 1957.
- ⁹Payne, F. M., "The Structure of Leading Edge Vortex Flows including Vortex Breakdown," Ph.D. Dissertation, Univ. of Notre Dame, Notre Dame, IN, 1987.
- ¹⁰Bergesen, A. J., and Porter, J. D., "An Investigation of the Flow around Slender Delta Wings with Leading Edge Separation," Princeton Univ. Aeronautical Engineering Rept. 510, Princeton, NJ, 1960.
- ¹¹Lowson, M. V., "The Separated Flows on Slender Wings in Unsteady Motion," Ph.D. Thesis, Dept. of Aeronautics and Astronautics, Univ. of Southampton, Southampton, England, UK, 1963.
- ¹²Werle, H., "Etude Physique des Phenomenes Tourbillonnaires au Tunnel Hydrodynamique," *Bull de l'Assoc. Tech. Maritime et Aeronautique*, Vol. 61, 1961, pp. 177-200.
- ¹³Werle, H., *Recherche Aeronautique*, ONERA, No. 109, 1965.
- ¹⁴Barsby, J. E., "Calculations of the Effect of Blowing from the Leading Edges of a Slender Delta Wing," Aeronautical Research Council, London, ARC R&M 3692, 1972.
- ¹⁵Lambourne, N. C., and Bryer, D. W., "The Bursting of Leading Edge Vortices—Some Observations and Discussions of the Phenomenon," Aeronautical Research Council, London, ARC R&M 3282, 1962.
- ¹⁶Gad-el-Hak, M., and Blackwelder, R. F., "The Discrete Vortices from a Delta Wing," *AIAA Journal*, Vol. 23, 1985, pp. 961-962.
- ¹⁷Payne, F. M., Ng, T. T., Nelson, R. C., and Schiff, L. B., "Visualization and Wake Surveys of Vortical Flow on a Delta Wing," *AIAA Journal*, Vol. 26, 1988, pp. 137-143.
- ¹⁸Winant, C. D., and Browand, F. K., "Vortex Pairing, the Mechanism for Turbulent Mixing Layer Growth at Moderate Reynolds Number," *Journal of Fluid Mechanics*, Vol. 63, 1974, pp. 237-255.
- ¹⁹Ho, C.-M., and Huerre, P., "Perturbed Free Shear Layers," *Annual Review of Fluid Mechanics*, Vol. 16, 1984, pp. 365-424.
- ²⁰Earnshaw, P. B., "An Experimental Investigation of the Structure of a Leading Edge Vortex," Aeronautical Research Council, London, ARC R&M 3281, 1962.
- ²¹Verhaagen, N. G., and Kruisbrink, A. C. H., "Entrainment Effect of a Leading Edge Vortex," *AIAA Journal*, Vol. 25, 1987, pp. 1025-1032.
- ²²Hall, M. G., "A Theory for the Core of a Leading Edge Vortex," *Journal of Fluid Mechanics*, Vol. 11, 1961, pp. 209-228.
- ²³Stewartson, K., and Hall, M. G., "The Inner Viscous Solution for the Core of a Leading Edge Vortex," *Journal of Fluid Mechanics*, Vol. 15, 1963, pp. 306-338.

Notice to Subscribers

We apologize that this issue was mailed to you late. The AIAA Editorial Department has recently experienced a series of unavoidable disruptions in staff operations. We will be able to make up some of the lost time each month and should be back to our normal schedule, with larger issues, in just a few months. In the meanwhile, we appreciate your patience.